Magnetic, thermodynamic, and transport characterization of $Na_{0.75}CoO_2$ single crystals

B. C. Sales, R. Jin, K. A. Affholter, P. Khalifah, G. M. Veith, and D. Mandrus
Condensed Matter Sciences Division, Oak Ridge National Laboratory, Oak Ridge, Tennessee 37831-6056, USA
(Received 13 February 2004; revised manuscript received 2 July 2004; published 15 November 2004)

The magnetic, thermal, and transport properties of $Na_{0.75}CoO_2$ single crystals grown by the floating zone (FZ) method are reported. Magnetic susceptibility, resistivity, magnetoresistance, and heat capacity data from these crystals indicate a bulk phase transition at $T_1=22$ K. These data are most consistent with the formation of an antiferromagnetic spin-density-wave (SDW) at 22 K with the easy axis for magnetization nearly along the **c** axis. Weak and soft ferromagnetism is observed for applied magnetic fields less than 0.5 Tesla, which is unusual for a SDW transition. The jump in the heat capacity at the SDW transition is 0.45 J/K-mol-Co, about 50% of the value expected from mean-field weak-coupling theory. The reduced jump and the decrease in the resistivity below T_1 are consistent with partial gapping of the Fermi surface. The magnetoresistance is small at the SDW transition but increases in both directions reaching a value of 100% at 2 K for applied fields of 8 Tesla. The magnetoresistance data imply that the mobility of the remaining carriers is large and increases below T_1. The observation of a SDW transition in this material is found to be sensitive to the preparation conditions and the degree of order in the Na layers. No SDW transition is observed in our polycrystalline powder with the same nominal composition ($Na_{0.75}CoO_2$) and lattice constants. Differential scanning calorimetry data, however, show distinct differences between the powder and crystal, suggesting a higher degree of order in the Na layers within the crystal. The crystal exhibits a sharp first-order phase transition at $T_2=340$ K, while for the powder this transition is smeared over the temperature range from 250 to 310 K.

DOI: 10.1103/PhysRevB.70.174419 PACS number(s): 75.30.Fv, 75.40.Cx

I. INTRODUCTION

The layered transition metal oxides, Na_xCoO_2, have been of considerable interest to the scientific community for the past few years. This family of materials has been known for some time[1] but the report by Terasaki *et al.*[2] concerning possible thermoelectric applications has rekindled interest in these compounds.[3–8] It is very unusual for an oxide to have a relatively high thermopower yet a low metallic resistivity.[9] This result alone suggests interesting electronic correlations. The subsequent discovery of superconductivity at 5 K by Takada *et al.*[10] in a hydrated version of this material ($Na_{0.35}CoO_2\cdot 1.3H_2O$) caused even greater excitement.[11–15] Although the superconducting transition temperature is too low for applications, the structural and chemical similarities between Na_xCoO_2 compounds and cuprate superconductors provide hope of additional insight into the physics of superconductivity in layered transition metal oxides. In Na_xCoO_2, the Co ions in each plane form a triangular lattice rather than the square lattice found in the cuprates. An $S=1/2$ triangular lattice is of great interest to theorists because of the inherent geometrical frustration of antiferromagnetic order and since Anderson's original RVB model for superconductivity[16] was calculated for a triangular lattice.

The basic structure of Na_xCoO_2 ($0.3<x<0.9$) consists of planes of edge-sharing CoO_6 octahedra alternating with layers of Na. In this article we focus on the most Na rich composition with the gamma phase: $Na_{0.75}CoO_2$. The gamma phase is hexagonal ($P6_3/mmc$) with $\mathbf{a}=2.83$ Å and $\mathbf{c}\approx 10.85$ Å. There are four crystallographically distinct positions within the unit cell: Co at (0,0,0.5), O at (0.333, 0.667, 0.0913), and two Na positions Na1 (0,0,0.25) and Na2 (0.667, 0.333, 0.25). Both Na positions are only partially occupied, and cannot be occupied randomly since that would result in some of the Na at site 1 being too close to Na at site 2.[6] One neutron structure refinement[17] estimates the average relative occupancy of Na1 ≈ 0.25 and Na2 ≈ 0.5. A Na at site 1 has a Co ion directly above and below it at a distance of 2.71 Å as compared to a Na2-Co minimum distance of 3.17 Å. In an ionic picture, the Co ions are mixed-valent with a formal oxidation state of 4-x. A simple electrostatic model would suggest that the Co near an occupied Na1 site would have a greater tendency toward Co^{+3}. Within this simple picture there are clearly tendencies toward some type of partial charge and Na ordering. This model is much too simple, however, since the overall electronic structure will also depend on the Na positions, as has recently been demonstrated by Huang *et al.*[18] Recent NMR data from $Na_{0.75}CoO_2$ powder, and resistivity, electron diffraction and neutron scattering data from $Na_{0.5}CoO_2$ crystals provide strong evidence of Na ordering near and above room temperature and charge order at lower temperatures.[19–21]

Magnetic data[22] and electronic structure calculations[6] suggests a low-spin configuration of $S=0$ for Co^{+3} and $S=1/2$ for Co^{+4} within a t_{2_g} ground state. Band structure calculations indicate that the six bands comprising the t_{2_g} manifold are split further in the rhombohedral crystal field into two a_{1_g} and four e_g^1 symmetry bands. At the Fermi energy most of the bands have a_{1_g} character with some e_g^1 admixture. The calculated Fermi surface has large cylindrical hole Fermi surfaces around the zone center (Γ) of dominant a_{1_g} character and small holelike sections with some e_g^1 character centered about 2/3 of the way out along the Γ-K and A-H directions. The large cylindrical Fermi surface is flattened along the Γ-K directions resulting in a cylinder with six facets (Allen wrench). Large portions of this Fermi sur-

face are susceptible to nesting.[6] In addition, because of two dimensionality, the smaller Fermi surface regions also have significant nesting[23] between themselves.

The present article focuses on the magnetic, transport, and thermodynamic properties of single crystals of $Na_{0.75}CoO_2$ grown by a floating zone method. Two distinct phase transitions are observed in these crystals, one at $T_1=22$ K and the other at $T_2\approx 340$ K. The transition at 22 K was first reported by Motohashi *et al.*[24] on powder samples of $Na_{0.75}CoO_2$ and later investigated by Sugiyama *et al.*[25] using muon spin rotation (μsr). Motohashi *et al.*[24] suggested that the transition at 22 K was likely a SDW, a conclusion consistent with the μsr results. The possibility of a SDW in similar materials was first pointed out by Terasaki[26] who reported a transition at 22 K in polycrystalline samples of $NaCo_{2-x}Cu_xO_4$. Very recent work[27] on Na_xCoO_2 crystals have also reported a magnetic transition near 22 K. A transition at $T_2\approx 340$ K has not been previously reported, although it is probably related to the smeared transition between 250–310 K studied by Gavilano *et al.*[20] on powder and the transition at ≈430 K observed by Wang *et al.*[28] in flux grown crystals.

II. SYNTHESIS AND EXPERIMENTAL METHODS

High purity powders of Na_2CO_3 (99.997% from Alfa-AESAR) and Co_3O_4 (99.999% from Alfa-AESAR) were carefully weighed to give the desired stoichiometry of $Na_{0.75}CoO_2$. The powders were first mixed by hand to yield a homogenous gray color and then ball milled for 2 h. The ball milled powder was loaded into a high purity (99.9%) alumina tray, inserted into a furnace that had been preheated to 750 °C and left for 20 h. This rapid-heat technique was found to minimize the loss of Na due to volatilization.[29] The prereacted powder (total weight of about 30 g) was pressed in to three 1 in. diameter pellets and placed on a thin layer of the same powder in an alumina tray. The pellets were heated to 830 °C for 16 h in pure O_2 that was slowly flowed over the tray (≈10 cm^3/min), and then cooled to room temperature over a period of 6–8 h. The final powder was obtained after ball milling all three pellets for an additional 1–2 h. Measurements of the weights before and after heat treatments indicated that the final stoichiometry was very close to $Na_{0.75}CoO_2$. Inductively-coupled-plasma-atomic-emission spectroscopy (ICP-AES) analysis of the powder gave a Na/Co ratio of 0.74 ± 0.02. Iodometric titration measurements gave a formal Co valence of 3.25 ± 0.01 in good agreement with the ICP and weight loss data. Powder x-ray diffraction showed only the desired hexagonal gamma phase $P6_3/mmc$ with $\mathbf{a}=2.83$ Å and $\mathbf{c}=10.86$ Å.

Single crystals with a composition close to $Na_{0.75}CoO_2$ were prepared from the $Na_{0.75}CoO_2$ powder using a floating zone method. The powder was hydrostatically compressed in rubber bladders into 6 mm diameter by 100 mm long rods. The fragile rods were carefully removed from the bladder, placed in an alumina tray on loose powder with the same composition, and heated at 830 °C for 16 h in flowing oxygen. The polycrystalline rods were used in an NEC SCM15-HD arc image furnace to prepare single crystals of $Na_{0.75}CoO_2$ via the floating zone method with typical growth rates of 2–5 mm/h. The material does not melt congruently and the formation of a single crystal free of Co_3O_4 and CoO impurities only occurs over the last 1–2 cm of a 10 cm feed rod. Although there was some Na lost, particularly during the initial stabilization of the molten zone, the crystal that was finally produced may have had slightly more Na than the starting feed rods due to the ability of the Na to move along the axis of the feed rod during growth. Laue x-ray photographs were used to cut or cleave oriented single crystal plates with typical dimensions of $5\times5\times1$ cm^3 from the as-grown boule. The crystal plates had lattice constants of $\mathbf{a}=2.83$ Å and $\mathbf{c}=10.82$ Å, very similar to the values found for the starting powder. ICP-AES analysis of the crystal gave a Na/Co ratio of 0.74 ± 0.03, also close to that of the powder. The crystals and powder were stored in sealed containers since the material would slowly react with moisture and CO_2 in the air. A small amount of white powder, identified as $Na_2CO_3\cdot yH_2O$, would sometimes form on the surface of a crystal left in ambient air for several days.

For comparison purposes, crystals of Na_xCoO_2 were grown from a NaCl flux in an alumina crucible as described in Ref. 5. These crystals typically contain small amounts of Al and perhaps other impurities. We found that the physical properties of the flux-grown crystals are significantly different at both low and high temperatures from crystals prepared with the floating zone method. The typical lattice constants from the flux grown crystals are $\mathbf{a}=2.83$ Å and $\mathbf{c}=10.92$ Å. The value for the **c** lattice constant indicates an average composition[19] of $Na_{0.72}CoO_2$.

We also tried to prepare powder with Na contents of $x=0.6$ and $x=0.67$ using the same protocol developed for preparing the $x=0.75$ powder. Both the $x=0.6$ and 0.67 powders showed significant amounts of Co_3O_4 either in the x-ray pattern or in the magnetic susceptibility data. If the powders are heated at still higher temperatures (≈900–950 °C) the Co_3O_4 impurity is converted or partially converted to a CoO impurity phase. We conclude that for synthesis methods in the 700–950 °C temperature range, the gamma phase only forms for a small range of Na concentrations $x=0.74\pm0.04$. Gamma phase samples of Na_xCoO_2 with lower concentrations of Na, however, can be prepared using nonequilibrium room temperature chemical or electrochemical extraction methods.[10,19,30]

As a further reproducibility check of the effect of the Na content on the lattice constants, a powdered sample of $Na_{0.37}CoO_2$ was prepared by stirring 8 g of the $Na_{0.75}CoO_2$ powder in a 6.6 M bromine/acetonitrile solution (15 cm^3 99.99% Br and 75 cm^3 99.999% CH_3CN) for 5 d. The powder, which is very hydroscopic, was thoroughly washed with pure CH_3CN and quickly transferred to a vacuum chamber where the small amount of remaining CH_3CN was pumped away resulting in a dry and fluffy powder. ICP and iodometric titration analysis of the powder yielded a Na content of $x=0.37\pm0.02$. Powder x-ray diffraction yielded $\mathbf{a}=2.83$Å and $\mathbf{c}=2.83$Å. This value for **c** is consistent with a Na content of $x=0.37$ reported in Ref. 19.

X-ray diffraction measurements were made with a Scintag PAD V powder diffractometer using Cu $K\alpha$ radiation. The fluorescence of Co atoms when exposed to Cu $K\alpha$ radiation significantly decreases the signal-to-noise ratio of the Bragg

peaks in powder patterns of compounds containing large amounts of Co. The fluorescence was greatly reduced, however, by a careful adjustment of the x-ray energy window (filter), which improved the signal-to-noise ratio by about a factor of 10 relative to the normal setting. Patterns were calibrated using an external LaB_6 standard through the JADE software package. The procedures used for the iodometric titration measurements have been described previously.[31] Scanning calorimetry measurements were made from 120–500 K using a Perkin-Elmer DSC-4. Magnetic susceptibility and magnetization data were collected using a commercial SQUID magnetometer from Quantum Design. Resistivity, heat capacity, thermal conductivity and Seebeck measurements were made using a Physical Property Measurement System (PPMS) from Quantum Design. To achieve a low contact resistance, gold pads ($\approx$1000 Å thick) were sputtered onto the crystals. Electrical leads were then attached to the gold pads using silver epoxy (H20E from EPOTEK).

III. MAGNETIC SUSCEPTIBILITY AND SCANNING CALORIMETRY

Magnetic susceptibility data are shown in Fig. 1 for the starting powder ($Na_{0.75}CoO_2$), floating zone (FZ) crystals ($Na_{0.75}CoO_2$) and flux grown crystals ($Na_{0.72}CoO_2$). For comparison purposes, the data for the crystals is the polycrystalline average for the two directions. These data illustrate how the properties of the material can vary with small changes in either Na stoichiometry or disorder within the Na layer. Only the susceptibility data from crystals prepared by the floating zone method show a clean magnetic transition at 22 K. For temperatures above 50 K, all of the susceptibility data in Fig. 1 can be parameterized by $\chi=\chi_o+C/(T+\theta)$. Least squares fits of the data gives effective moments of 1.12–1.36 μ_B per Co, and values of χ_o between 1.36×10^{-4} and 1.71×10^{-4} cm^3/mol. The constant χ_o accounts for Pauli paramagnetism and core diamagnetism. The values for θ, are 120 K, 122 K, and 206 K for the powder, flux-grown crystal, and FZ crystal, respectively. The larger value of θ for crystals grown by the floating zone method may be related to a higher degree of Na order as discussed below.

Since the powder and FZ crystals have virtually identical chemical compositions, the likely origin of the difference in the magnetic properties is the degree or type or order in the Na layers between the CoO_2 planes. An initial analysis of x-ray powder diffraction data showed no obvious structural differences between the two materials, but further structural studies are clearly needed. We note that recently other authors have found similar differences in properties between powder and crystals of Na_xCoO_2 with similar compositions.[32] Scanning calorimetry data, however, showed clear differences. The powder exhibited two to four distinct endothermic peaks when heating through the temperature range from 250 to 310 K. The approximate positions and magnitude of each peak were reproducible for different powder samples and for subsequent scans of the same powder. The heat associated with each peak ranged from $\approx$40 to 160 J/mol $Na_{0.75}CoO_2$. In the gamma structure

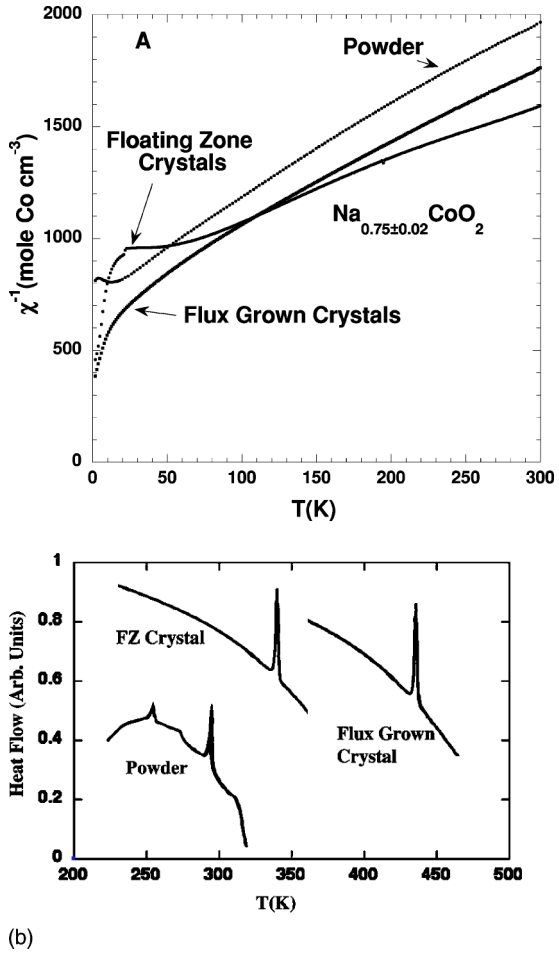

FIG. 1. (a) Inverse magnetic susceptibility vs temperature for three samples of $Na_{0.75\pm0.02}CoO_2$ prepared by different methods. These data were taken in an applied field of 0.1 Tesla. The data shown are field cooled (FC), although at this field there is no significant difference between FC and zero-FC. The susceptibility data are given in units of cm^3/mol-Co that is often written in the literature as emu/mole. To convert to emu/g, the susceptibility values in the figure should be divided by the molecular weight of 108 g/mol. (b) DSC scans from the same three samples.

there are two crystallographically distinct Na sites with each site only partially occupied.[17] It is likely that the endothermic peaks correspond to a rearrangement of the Na within each layer. DSC measurements on the FZ crystals showed only one sharp endothermic peak at 343 K on heating with a total latent heat of about 700 J/mol $Na_{0.75}CoO_2$. The transition at 343 K was hysteretic and was about 6° lower on cooling, indicating a first order phase transition. Measurements on several different crystals indicated a one-to-one correspondence between a sharp DSC peak at 343 K and a distinct magnetic transition at 22 K. DSC measurements were also performed on several flux grown crystals ($Na_{0.75}CoO_2$). These crystals exhibited a sharp endothermic peak at 430 K with a heat content of about 1000 J/mol. However, there was no distinct magnetic transition for these crystals, possibly because these crystals had a lower Na content. DSC measurements on the $Na_{0.37}CoO_2$ powder showed no thermal anomaly in the temperature range from 120 to 500 K.

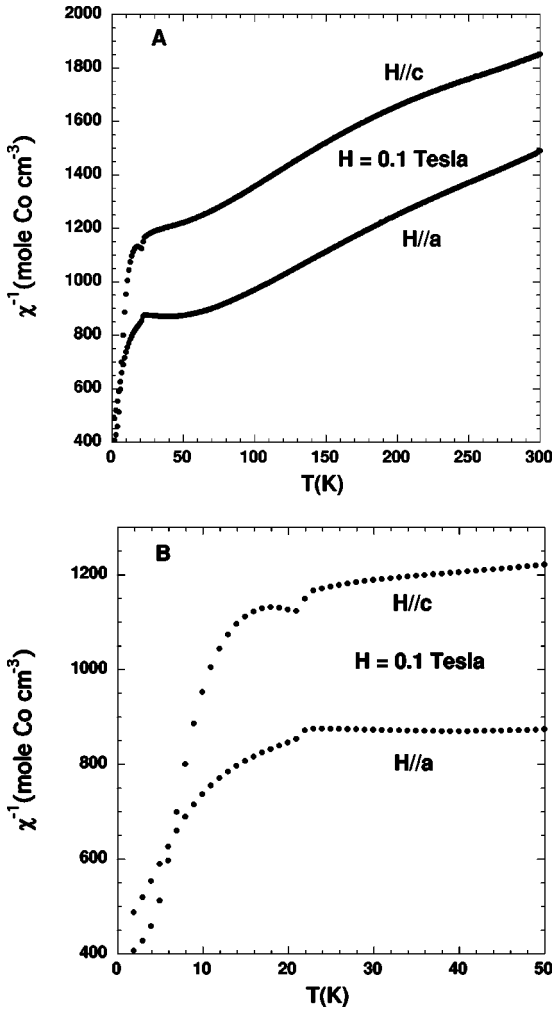

FIG. 2. (a) Inverse magnetic susceptibility (FC) vs temperature for a $Na_{0.75}CoO_2$ crystal grown via the floating zone method. (b) Low temperature plot of same data. A magnetic transition at 22 K is evident for $H\|a$ and $H\|c$.

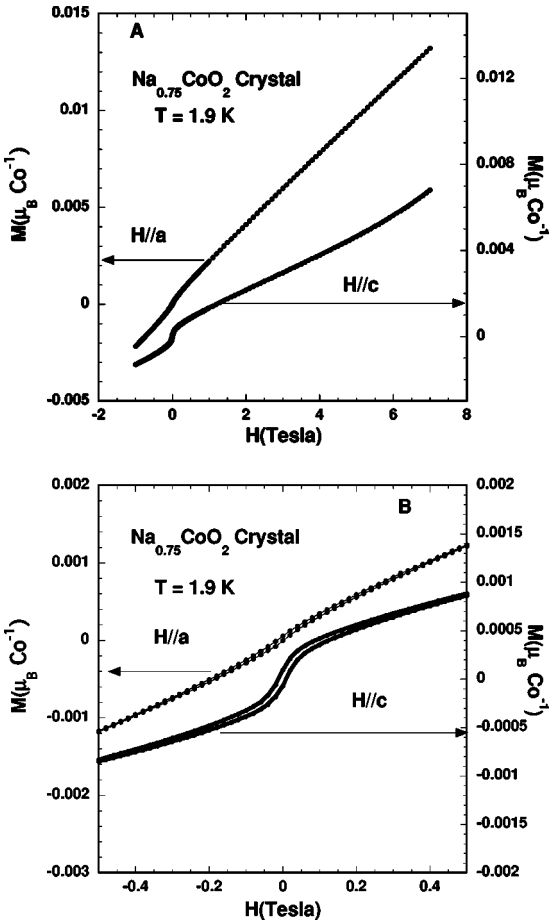

FIG. 3. (a) Magnetization vs field at $T=1.9$ K for a $Na_{0.75}CoO_2$ crystal grown via the floating zone method. Very weak ferromagnetic behavior is evident for $H<0.5$ Tesla. At higher fields the magnetization data are more consistent with a type of antiferromagnetic order. (b) Low field plot of same data.

Very recent work by Huang *et al.*[33] confirm this interpretation. They find that there is a structural phase transition in Na_xCoO_2 near $x=0.75$ due to Na rearrangement. Crystals with $x\approx 0.75$ grown via the FZ method were found to have a more ordered Na arrangement at room temperature, but converted to a more disordered phase at $T\approx 320$ K. Polycrystalline powder with virtually the same Na content tended to form in the more disordered phase (Na at the Na2 site appears to move off center to one of three nearby positions).

The remainder of this article will focus on the properties of $Na_{0.75}CoO_2$ crystals prepared using the floating zone method and the nature of the magnetic transition at 22 K and the Na ordering transition at 343 K. The magnetic susceptibility data for magnetic fields applied parallel to **a** and **c** are displayed in Fig. 2. On cooling there is a clear and abrupt increase in the susceptibility in both directions at $T_1=22$ K in a field of 0.1 Tesla. This transition was first reported by Motahashi *et al.*[24] in $Na_{0.75}CoO_2$ powder. Above 50 K the susceptibility data in Fig. 2 can be parameterized by $\chi=\chi_o+C/(T+\theta)$ with $\chi_o=9.49\times10^{-5}$ cm^3/mol Co, $p_{\text{eff}}=1.56$ μ_B, and $\theta=220$ K for $H\|\mathbf{a}$ and $\chi_o=2.76\times10^{-4}$ cm^3/mol Co, $p_{\text{eff}}=1$ μ_B, and $\theta=167$ K for $H\|\mathbf{c}$. The anisotropy in the susceptibility data is significant ranging from 25% at 300 K to 45% at 50 K. The flattening (saturation) of the susceptibility data for temperatures between 50 K and 22 K (for both the powder and FZ crystal) may be due to 2D antiferromagnetic correlations within the CoO_2 layers. Magnetization data at 1.9 K are shown in Fig. 3 for $H\|\mathbf{a}$ and $H\|\mathbf{c}$. In both directions there is evidence of weak ferromagnetism and hysteresis for applied magnetic fields of less than 0.5 Tesla. The remanent magnetization is very small and corresponds to about 0.0001 μ_B per Co for $H\|\mathbf{c}$ and less for $H\|\mathbf{a}$. The coercive field is about 100 Oe. The ferromagnetic hysteresis is absent above 22 K. For applied fields larger than 1 or 2 Tesla the magnetization is linear in field for $H\|\mathbf{a}$ and nearly linear for $H\|\mathbf{c}$. The magnetization data for $H\|\mathbf{c}$ begins to curve upwards for $H>5$ T, which suggests a possible metamagnetic transition at fields greater than 7 Tesla (the limit of our instrument). The extremely small magnetization associated with the ferromagnetic behavior at low fields, coupled with the linear and superlinear behavior of the magnetization at higher fields suggests that ferromagnetism is not the dominant magnetic response of the system. To test this hypothesis the susceptibility of $Na_{0.75}CoO_2$ was measured in

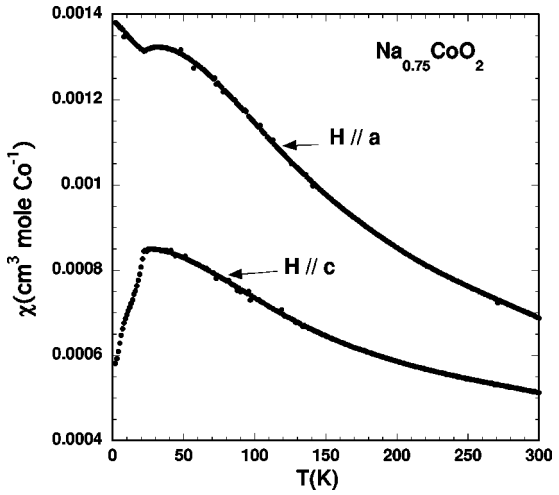

FIG. 4. Susceptibility vs temperature with an applied field of 5 Tesla.

an applied field of 5 Tesla (Fig. 4). The susceptibility data resembles that of an antiferromagnet[34] with the magnetic spins aligned along the **c** axis of $Na_{0.75}CoO_2$. The increase in the susceptibility in low magnetic fields for temperatures below 22 K for $H\|\mathbf{a}$, and $H\|\mathbf{c}$ however, suggests that the magnetic response of this material is complex. We are not aware of a SDW material (or any metallic antiferromagnetic material) that exhibits both weak and soft ferromagnetism similar to that found for $Na_{0.75}CoO_2$ crystals. Preliminary neutron scattering measurements[35] on a 1 cm^3 single crystal found no evidence of a commensurate magnetic structure. For comparison, the magnetization data at 1.9 K for the $Na_{0.75}CoO_2$ powder (not shown) is perfectly linearly for fields from 0 to 7 Tesla.

Magnetic susceptibility data were also taken for temperatures between 300 and 400 K to see if the structural transition at 340 K had a magnetic signature. There was a very small increase (jump of about 1%) in the magnetic susceptibility on cooling below 340 for $H\|\mathbf{c}$ (Fig. 5) and an even smaller effect for $H\|\mathbf{a}$.

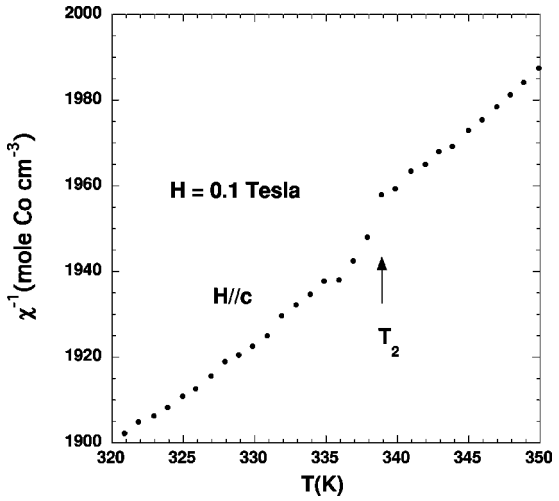

FIG. 5. Inverse susceptibility of $Na_{0.75}CoO_2$ vs temperature in the vicinity of T_2. There is about a 1% change in χ near T_2.

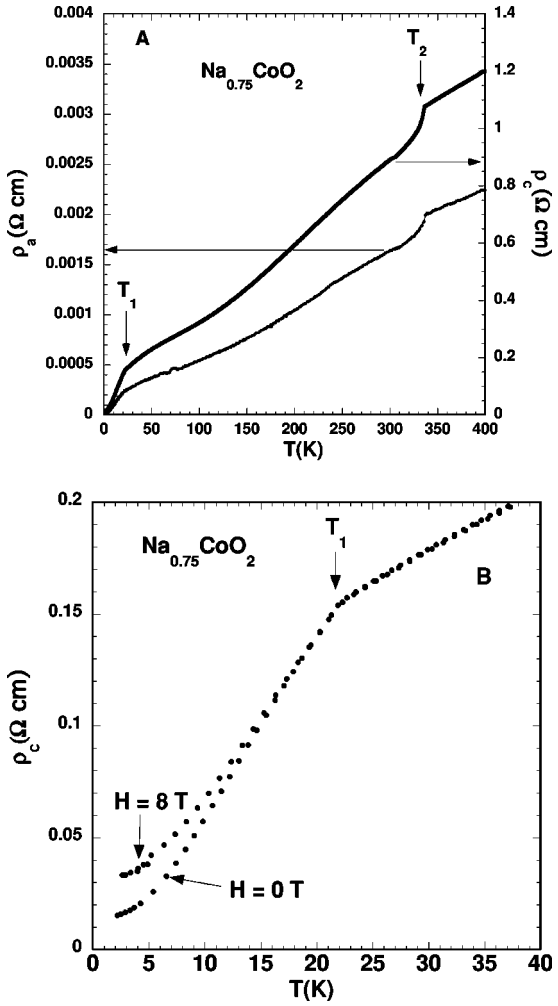

FIG. 6. (a) Resistivity of a $Na_{0.75}CoO_2$ crystal for current in the plane (ρ_a) and along the c axis (ρ_c). The magnetic transition at $T_1 = 22$ K and the ordering transition at $T_2 = 340$ K are evident in the resistivity data. (b) Low temperature resistivity data (ρ_c) vs temperature in 0 and an 8 Tesla field ($H\|c$). Similar but noisier data were also found for ρ_a with $H\|c$.

IV. RESISTIVITY AND MAGNETORESISTANCE

The temperature dependence of the resistivity data is shown in Fig 6(a). Both the in-plane, ρ_a, and out-of-plane, ρ_c, resistivities are metallic over the entire temperature range (2–400 K) with ρ_c about 600 times larger than ρ_a. The first-order transition at 340 K (T_2) and the magnetic transition at 22 K (T_1) are clearly evident in the resistivity data. Cooling the crystal through each transition results in an abrupt decrease in the resistivity. By 2 K the resistivity in both directions is 10 times smaller than the value extrapolated from data above 22 K. This strongly suggests that the magnetic phase transition that occurs at T_1 is a bulk effect and is not due a small amount of a magnetic impurity phase. The magnetoresistance is small near T_1 but rapidly increases as the temperature is reduced further [Fig. 6(b)]. For local-moment type magnets the magnetoresistance is maximal near the ordering temperature,[36] in sharp contrast to the behavior of $Na_{0.75}CoO_2$. The field dependence of ρ_c at 2 and 5 K for $H\|\mathbf{c}$

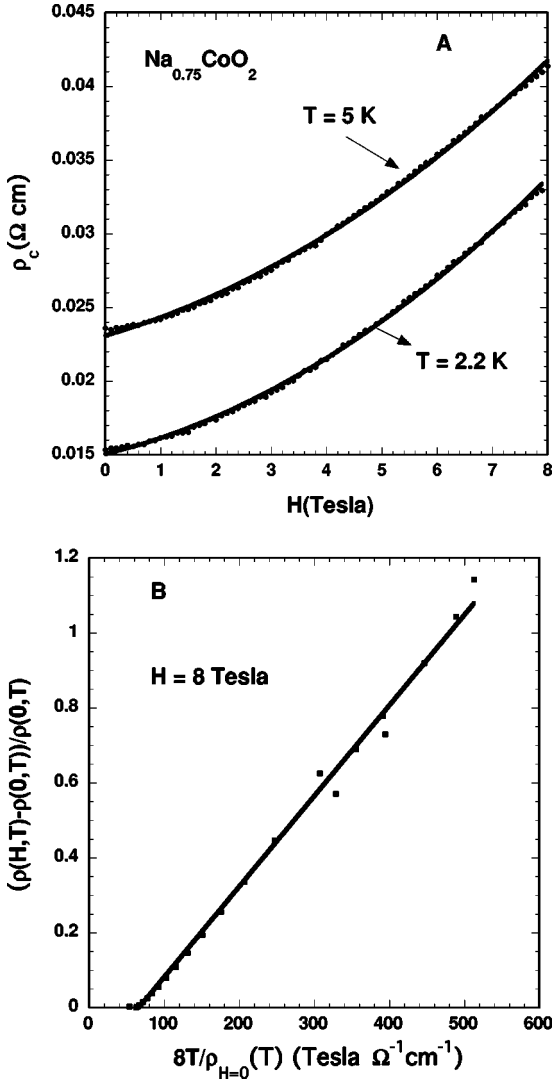

FIG. 7. (a) Resistivity (ρ_c) vs magnetic field ($H\|c$) at $T=2.2$ and $T=5$ K. (b) Magnitude of magnetoresistance at 8 Tesla vs conductivity at zero field $(1/\rho(T)_{H=0})$. These data suggest that the large magnetoresistance at low temperatures is due to an increase in the mobility of the carriers as the temperature is lowered below T_1.

is shown in Fig 7(a). At 2 K a field of 8 T more than doubles the resistivity. In spite of the large magnetoresistance at low temperatures, a field of 8 T has no detectable effect on the transition temperature of 22 K. In "normal" metals the magnitude of the magnetoresistance increases quadratically with magnetic field in a manner similar to that observed in Fig. 7(a). These data do not show any clear evidence of an incipient metamagnetic transition that was suggested from the magnetization data [Fig. 3(a)]. The magnetoresistance of "normal" metals also increases as the mobility of the carriers increases (or as the resistivity decreases). We show in Fig. 7(b) that the longitudinal magnetoresistance below T_1 scales as the conductivity in zero field $(1/\rho(0,T))$. Similar behavior was observed at 2 and 5 K for ρ_a with $H\|\mathbf{c}$ (transverse magnetoresistance). These data suggest that the large magnetoresistance below T_1 is due to an increase in carrier mobility. A more complete study of the low temperature magnetotransport properties of $Na_{0.75}CoO_2$ crystals is in progress.

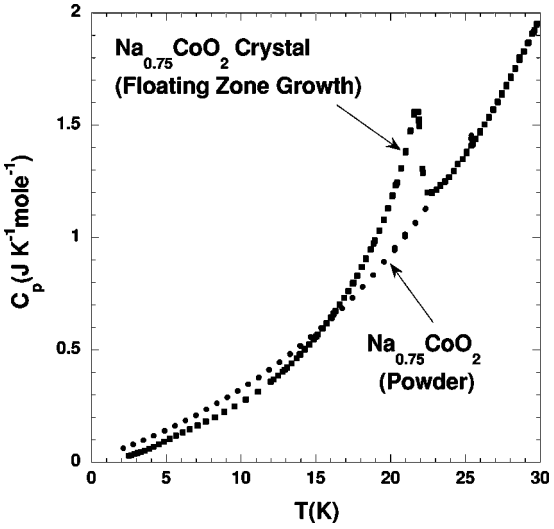

FIG. 8. Heat capacity vs temperature for a crystal prepared via the floating zone method and a powder with essentially the same composition. The only significant difference between the two samples appears to be the degree of order in the Na layers. This difference is clearly reflected in the DSC data shown in Fig. 1(b).

V. HEAT CAPACITY

Heat capacity data versus temperature for a $Na_{0.75}CoO_2$ crystal and for the $Na_{0.75}CoO_2$ starting powder are shown in Fig. 8. As discussed previously, we believe that the only significant difference between the powder and the crystal is the degree of order in within the Na layers. The heat capacity data from the crystal exhibits a distinct transition at 22 K that is very similar in shape to the heat capacity anomaly from a BCS superconductor. The heat capacity data from the powder exhibits no phase transition in the temperature range from 5 to 30 K and can be accurately described as a sum of an electronic and lattice contribution ($C_{\text{powder}}=\gamma T+\beta T^3$) with $\gamma=0.027$ J/K^2-mol-Co and $\beta=4.34\times10^{-5}$ J/K^4-mol-Co. This value for β implies a Debye temperature, θ_D, of 545 K. The values for γ and θ_D are similar to the values estimated by Motohashi *et al.*[24] The data from the powder was scaled by a few percent to exactly match the heat capacity of the crystal at 30 K, compensating for the weighing errors of 2%–5%. The entropy associated with the magnetic transition is estimated to be only 0.08 J/(mol-Co K). If this transition corresponded to the long range magnetic ordering of localized Co^{+4} spins, we would expect the entropy associated with the transition to be of order $0.25R\ln(2)$ ≈ 1.44 J/mol-Co-K, which is 20 times larger than found experimentally. Short range correlations could remove part of the entropy at higher temperatures (below 50 K where the susceptibility flattens) but it seems unlikely that 95% was removed at higher temperatures. The magnitude and shape of the heat capacity feature near 22 K (Fig. 8), however, is consistent with the formation of a gap over part of the Fermi surface as a result of the development of a spin-density-wave (SDW). In the simplest models of a SDW, the transition is considered to involve only the electrons near the Fermi energy. The lattice contribution to the heat capacity from the crystal was estimated using the data from the powder, which

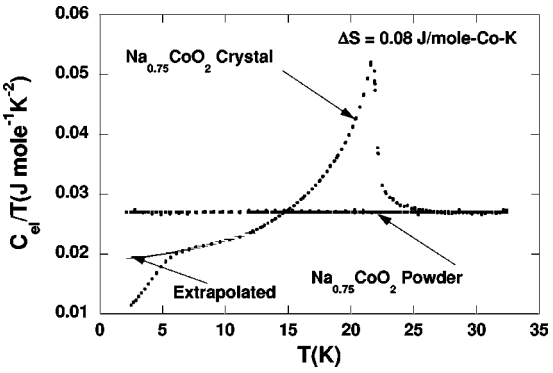

FIG. 9. Electronic portion of the heat capacity divided by temperature vs temperature for the crystal and the powder. The shape of the peak in the heat capacity data and the magnitude of the entropy associated with the transition at 22 K strongly imply the formation of a SDW. The downturn in C_{el}/T at about 6 K for the data from the crystal is of unknown origin and may be extrinsic or intrinsic. The extrapolated behavior shown for C_{el}/T is consistent with the conservation of entropy for the main transition.

does not show a transition. The electronic portion of the heat capacity divided by T (C_{el}/T) for the crystal and the powder are shown in Fig. 9. For a SDW, the net entropy change below 22 K associated with the transition must coincide with the entropy reduction if the electronic density of states maintains its value just above the transition (γ=0.027 J/K^2-mol-Co) all the way to T=0. This constraint[37] means that the area of the peak with $C_{el}/T > \gamma$ has to equal the area where $C_{el}/T < \gamma$. Based on this constraint we conclude that the downturn at about 6 K in the C_{el}/T data from the crystal is not associated with the main SDW transition. The downturn in C_{el}/T below 6 K may be extrinsic or intrinsic, but we have no good explanation for the data. The expected behavior of C_{el}/T below 6 K due to the SDW transition is sketched in Fig. 9. This extrapolation is consistent with the entropy constraint. The jump in the electronic portion of the heat capacity at the SDW transition is ΔC=0.45 J/(mol-CoK) and hence $\Delta C/\gamma T_{SDW}$=0.75. We note that γ contains contributions from both the large and small pockets of the Fermi surface. Because of different effective masses, each portion of the Fermi surface contributes about half of the measured density of states above the transition.[38] Mean-field weak-coupling-limit theory predicts that this ratio should be the same as that for a BCS superconductor,[39] $\Delta C/\gamma T_{SDW}$=1.43. Since the resistivity data clearly indicate that the entire Fermi surface is not gapped, the ratio 0.75/1.43=0.52 can be used as a crude estimate of the fraction of the Fermi surface affected by the SDW transition. The heat capacity of the crystal was also measured in a field of 8 T with $H \| \mathbf{c}$ (not shown). There was no detectable effect of a magnetic field on the data shown in Fig. 8.

VI. THERMAL CONDUCTIVITY AND THERMOPOWER

The thermal conductivity, κ_a, and thermopower, S, data from a $Na_{0.75}CoO_2$ crystal are shown in Figs. 10 and 11 with

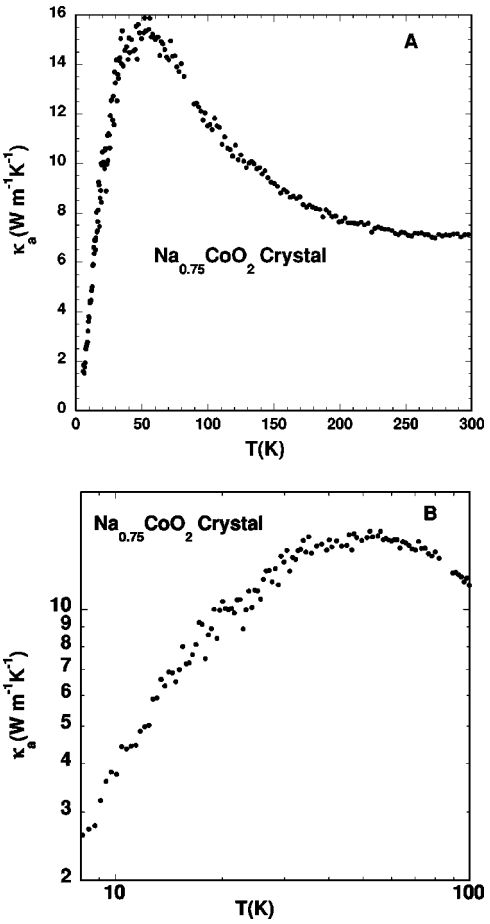

FIG. 10. (a) In-plane thermal conductivity, κ_a vs temperature for a $Na_{0.75}CoO_2$ crystal. (b) Log of κ_a vs log of temperature. Notice that there is no clear sign of the SDW transition at 22 K in the thermal conductivity data. This result implies weak coupling between the conduction electrons involved in the SDW transition and the acoustic phonons that carry most of the heat.

the temperature gradient and heat flow along the **a** axis. The temperature dependence of the thermal conductivity data [Fig. 10(a)] is typical of an insulating crystal. The electronic contribution, κ_e, to the thermal conductivity can be estimated using the Wiedemann-Franz Law and the resistivity data shown in Fig. 6(a). κ_e is 0.4 W/m-K at 300 K and 0.24 W/m-K at 10 K. These values are less than 10% of the measured thermal conductivity, which means that most of the heat in these crystals is carried by phonons. The lack of a clear anomaly at 22 K implies relatively weak coupling between acoustic phonons that carry most of the heat and the electrons involved in the SDW transition. As has been pointed out by several authors[2,8] the thermopower of $Na_{0.75}CoO_2$ near room temperature is unusually high ($S \approx 115\ \mu$V/K) for a metal, which has led to interest is this and related layered CoO_2 compounds for thermoelectric applications. The rearrangement of the electronic structure that occurs near the SDW transition at 22 K has a clear impact on the thermopower below 22 K. A qualitative discussion of S

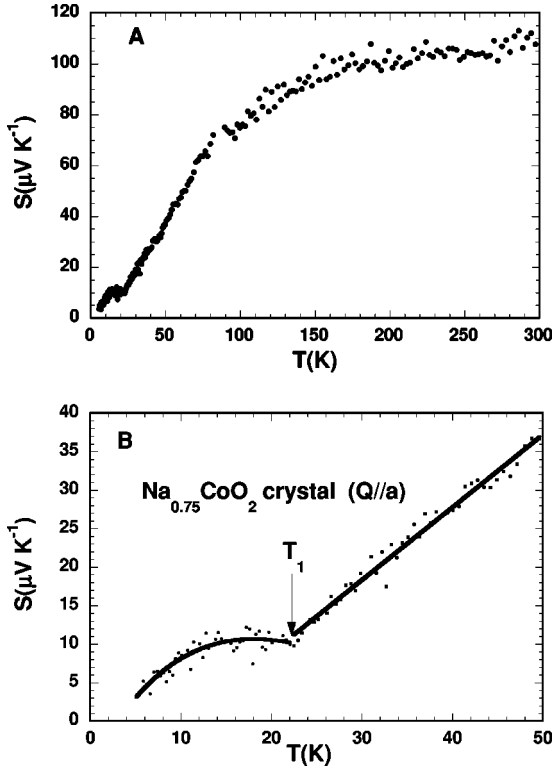

FIG. 11. (a) Thermopower, S, vs temperature. The value of S at high temperatures is unusually high for a metal, which has attracted interest in this material for thermoelectric applications (Refs. 2 and 3). (b) The SDW transition at $T_1 = 22$ K has a clear effect on the temperature dependence of the thermopower, consistent with a change in the Fermi surface.

below 22 K, however, requires detailed knowledge of the new electronic structure.

VII. EVIDENCE OF A SDW TRANSITION

The magnetic susceptibility data (Figs. 2–4) for the $Na_{0.75}CoO_2$ crystal exhibits a clear magnetic transition at 22 K. These data are consistent with either local-moment canted antiferromagnetism or an unusual SDW. The heat capacity data shown in Figs. 8 and 9 indicate that the entropy removed as a result of the magnetic transition is at least 20–50 times smaller than expected from a simple local moment interpretation ($\Delta S \approx R \ln 2$), arguing against the local moment picture. The shape of the heat capacity anomaly near 22 K is exactly what would be expected for a SDW transition. While it might be possible to interpret the magnetic and heat capacity data as a local moment transition from an undetected impurity phase in the crystal, the resistivity data shown in Figs. 6 and 7 rule out this interpretation. The large drop in the resistivity below 22 K is difficult to reconcile with an impurity-phase scenario. The large increase in the magnetoresistance as the sample is cooled below the transition is also not expected from a local moment antiferromagnetic transition. For such materials the magnetoresistance is normally largest near the transition but decreases in magnitude as the temperature is lowered further. Taken together, the magnetic susceptibility, heat capacity, resistivity and magnetoresistance data from the $Na_{0.75}CoO_2$ crystal provide strong evidence for a SDW transition. The calculated Fermi surface[6] provides a natural explanation for both the presence of a SDW and the decrease in the resistivity of $Na_{0.75}CoO_2$ below the transition (Fig. 6). As discussed in the Introduction, the calculated Fermi surface has two holelike parts. The larger portion of the Fermi surface consists of a faceted cylinder (allen wrench) of mainly a_g character. The smaller holelike sections have both a_g and $e_g{}^1$ character. Nesting and the formation of a SDW are most likely to occur for the smaller holelike sections.[23] Holes from the smaller holelike portions of the Fermi surface have high effective masses and may act as strong scattering centers for the lighter carriers from the allen wrench portion of the Fermi surface. This scenario would explain why the resistivity decreases below 22 K even though the total number of carriers is lower. We note that resistivity and magnetoresistance data[40] from the well studied SDW material $FeGe_2$ are similar to the data presented here for $Na_{0.75}CoO_2$.

VIII. SUMMARY AND CONCLUSIONS

The properties of $Na_{0.75}CoO_2$ are sensitive to the details of sample preparation. Polycrystalline powder and single crystals of $Na_{0.75}CoO_2$ with the same nominal compositions and lattice constants exhibit qualitatively different properties. The FZ crystals exhibit a SDW transition at 22 K, and a sharp first order transition at about 340 K with a latent heat of 700 J/mol. The powder shows no magnetic transition above 2 K and the first order transition at higher temperatures is smeared over the temperature range from 250 to 310 K as a series of first order transitions with latent heats ranging from 40 to 160 J/mol. The variation in properties is likely related to the distribution of Na in each Na layer. Very recent neutron diffraction results by Huang *et al.*[33] confirm this hypothesis. As to the low temperature ground state, LSDA calculations predict a weak ferromagnetic instability, but Singh[6] notes that close in energy there are "a large space of spin and charge orderings that are nearly degenerate with each other."

The FZ crystals exhibit a phase transition at $T_1 = 22$ K. Heat capacity, magnetization, resistivity, and magnetoresistance data indicate a SDW phase transition at 22 K from a gap that develops over only a portion of the Fermi surface. The heat capacity data exhibit a feature at 22 K that is very similar in shape to the heat capacity peak from a BCS superconductor. The entropy associated with the transition is small, only 0.08 J/(K mol-Co). The jump in the heat capacity at T_1 is 0.45 J/(K mol-Co) or about 50% of the value expected from mean-field theory. Low and high field magnetization data indicate that the easy axis for the spin density magnetization is nearly along **c**. Upward curvature in the high-field magnetization data at 2 K implies that a metamagnetic transition may occur for $H \| \mathbf{c}$ for fields higher than 7 T (the limit of our instrument). Weak and soft ferromagnetism for fields less than 0.5 T is very unusual in a SDW transition. Preliminary neutron scattering measurements[35] on a 1 cm^3 single crystal found no evidence of a commensurate

magnetic structure. The temperature of the SDW ($T_1 = 22$ K) transition is not changed in an 8 T magnetic field, but there is a large magnetoresistance at low temperatures; the resistivity at 2 K doubles in a field of 8 T. The resistivity in both directions (ρ_a, ρ_c) decreases more rapidly below 22 K than expected from an extrapolation of the resistivity data above 22 K.

ACKNOWLEDGMENTS

It is a pleasure to acknowledge stimulating discussions with David Singh and Stephen Nagler. Oak Ridge National Laboratory is managed by UT-Battelle, LLC, for the U.S. Department of Energy under Contract No. DE-AC05-00OR22725.

[1] C. Fouassier, G. Matejka, J.-M. Reau, and P. Hagenmuller, J. Solid State Chem. **6**, 532 (1973).
[2] I. Terasaki, Y. Sasago, and K. Uchinokura, Phys. Rev. B **56**, R12 685 (1997).
[3] K. Fujita, T. Mochida, and K. Nakamura, Jpn. J. Appl. Phys., Part 1 **40**, 4644 (2001).
[4] Y. Ando, N. Miyamoto, K. Segawa, T. Kawata, and I. Terasaki, Phys. Rev. B **60**, 10 580 (1999).
[5] M. Mikami, M. Yoshimura, Y. Mori, T. Sasaki, R. Funahashi, and I. Matsubara, Jpn. J. Appl. Phys., Part 1 **41**, L777 (2002).
[6] D. Singh, Phys. Rev. B **61**, 13 397 (2000).
[7] Y. Wang, N. S. Rogado, R. J. Cava, and N. P. Ong, Nature (London) **423**, 425 (2003).
[8] W. Koshibae, K. Tsutsui, and S. Maekawa, Phys. Rev. B **62**, 6869 (2000).
[9] G. D. Mahan, B. C. Sales, and J. W. Sharp, Phys. Today **50**, 42 (1997).
[10] K. Takada, H. Sakurai, E. Takayama-Muromachi, F. Izumi, R. A. Dilanian, and T. Sasaki, Nature (London) **422**, 53 (2003).
[11] R. Jin, B. C. Sales, P. Khalifah, and D. Mandrus, Phys. Rev. Lett. **91**, 217001 (2003).
[12] B. Kumar and B. S. Shastry, Phys. Rev. B **68**, 104508 (2003).
[13] J. D. Jorgensen, M. Avdeev, D. G. Hinks, J. C. Burley, and S. Short, Phys. Rev. B **68**, 214517 (2003).
[14] H. Sakurai, K. Takada, S. Yoshii, T. Sasaki, K. Kindo, and E. Takayama-Muromachi, Phys. Rev. B **68**, 132507 (2003).
[15] R. E. Schaak, T. Klimczuk, M. L. Foo, and R. J. Cava, Nature (London) **424**, 527 (2003).
[16] P. W. Anderson, Mater. Res. Bull. **8**, 153 (1973).
[17] R. J. Balsys and R. L. Davis, Solid State Ionics **93**, 2279 (1996).
[18] Q. Huang, M. L. Foo, R. A. Pascal Jr., J. W. Lynn, B. H. Toby, T. Hao, H. W. Zandbergen, and R. J. Cava, cond-mat/040404 (unpublished).
[19] M. L. Foo, Y. Wang, S. Watauchi, H. W. Zandbergen, T. He, R. J. Cava, and N. P. Ong, Phys. Rev. Lett. **92**, 247001 (2004).
[20] J. L. Gavilano, D. Rau, B. Pedrini, J. Hinderer, H. R. Ott, S. M. Kazakov, and J. Karpinski, Phys. Rev. B **69**, 100404 (2004).
[21] H. W. Zandbergen, M. L. Foo, Q. Xu, V. Kumar, and R. J. Cava, Phys. Rev. B **70**, 024101 (2004).
[22] R. Ray, A. Ghoshray, K. Goshray, and S. Nakamura, Phys. Rev. B **59**, 9454 (1999).
[23] M. D. Johannes, I. I. Mazin, D. J. Singh, and D. A. Papaconstantopoulos, cond-mat/0403135 (unpublished).
[24] T. Motohashi, R. Ueda, E. Naujalis, T. Tojo, I. Terasaki, T. Atake, M. Karppinen, and H. Yamauchi, Phys. Rev. B **67**, 064406 (2003).
[25] J. Sugiyama, H. Itahara, J. H. Brewer, E. J. Ansaldo, T. Motohashi, M. Karppinen, and H. Yamauchi, Phys. Rev. B **67**, 214420 (2003).
[26] I. Terasaki, I. Tsukada, and Y. Iguchi, Phys. Rev. B **65**, 195106 (2002).
[27] S. Bayrakci, C. Bernhard, D. P. Chen, B. Keimer, R. K. Kremer, P. Lemmens, C. T. Lin, C. Niedermayer, and J. Strempfer, Phys. Rev. B **69**, 100410 (2004).
[28] Y. Wang, N. S. Rogado, R. J. Cava, and N. P. Ong, cond-mat/0305455 (unpublished).
[29] T. Motohashi, E. Naujalis, R. Ueda, K. Isawa, M. Karppinen, and H. Yamauchi, Appl. Phys. Lett. **79**, 1480 (2001).
[30] F. C. Chou, J. H. Cho, P. A. Lee, E. T. Abel, K. Matan, and Y. S. Lee, Phys. Rev. Lett. **92**, 157004 (2004).
[31] F. Licci, G. Turilli, and P. Ferro, J. Magn. Magn. Mater. **164**, L268 (1996).
[32] D. Prabhakaran, A. T. Boothroyd, R. Coldea, L. M. Helme, and D. A. Tennant, cond-mat/0312493 (unpublished).
[33] Q. Huang, B. Khaykovich, F. C. Chou, J. H. Cho, J. Lynn, and Y. S. Lee, cond-mat/0405677 (unpublished).
[34] C. Kittel, *Introduction to Solid State Physics*, 3rd ed. (Wiley, New York, 1968), p. 484.
[35] Stephen Nagler (private communication).
[36] B. C. Sales, B. C. Chakoumakos, R. Jin, J. R. Thompson, and D. Mandrus, Phys. Rev. B **63**, 245113 (2001).
[37] A. Arrott, in *Magnetism*, edited by G. T. Rado and H. Suhl (Academic, New York, 1966), Vol. IIB, p. 325.
[38] D. J. Singh (private communication).
[39] G. Gruner, Rev. Mod. Phys. **66**, 1 (1994).
[40] C. P. Adams, T. E. Mason, S. A. M. Mentink, and E. Fawcett, J. Phys.: Condens. Matter **9**, 1347 (1997).